Performance of a Low-Power One-Way Travel-Time Inverted Ultra-Short Baseline Navigation System

Michael V. Jakuba*, James W. Partan*, Sarah E. Webster†, Dennis Giaya*, and Christina Ramirez†
*Woods Hole Oceanographic Institution, Woods Hole, MA USA
†Applied Physics Laboratory, University of Washington, Seattle, WA USA

***Abstract*—We report the performance of a low-power one-way travel-time inverted ultra-short baseline (OWTTIUSBL) system designed specifically for use on long endurance autonomous underwater vehicles (AUVs), as deployed during trials in late 2020. The system consists of a WHOI Micromodem-2 as the acoustic processing core coupled with a MEMS attitude and heading reference system (AHRS) and bespoke four-channel array. At low tilts our system provides standalone position fixes to better than $\pm 5^\circ$ azimuth at slant ranges in excess of 1500 m. The system consumes 1.1 W when active and is capable of entering a low-power 10 mW sleep mode sufficient to maintain its time base. These specifications are based on data collected with the device lowered from a vessel and excited by a mobile source on the vessel's small boat. We further present preliminary results from the device as installed on a Seaglider that show the potential for improved low-power navigation insensitive to temporal or depth-dependent variations in current profile.**

I. Introduction

Ongoing development efforts promise to deliver long endurance and deep-diving gliders with the potential to persistently observe the deep (6000 m) ocean interior and sea floor over time scales of months to years. These assets and their shallow-diving (<1000 m) predecessors navigate primarily by dead-reckoning between surfacing for GPS fixes, a paradigm that precludes their use in missions where science objectives call for precise navigation deep in the water column or near the deep sea floor. Coupled with a single autonomous surface vessel (ASV), OWTTIUSBL offers a compelling alternative to infrastructure-intensive external acoustic aiding. Such systems could provide navigation aiding to multiple underwater vehicles while retaining a level of autonomy and endurance for the system as a whole comparable to that of a solitary vehicle.

A glider's navigational accuracy depends chiefly on how long it spends submerged between global positioning system (GPS) fixes, and secondly on the strength and variability of the background water current profile. This kind of navigation is entirely standalone. OWTTIUSBL provides a position fix whose accuracy is primarily a function of distance to the acoustic source. The quality of the fix is not dependent on time and is unaffected by the current profile; however, OWTTIUSBL imposes a maximum range between the glider and an acoustic source with access to GPS or other high resolution positioning information. Our system provides standalone position fixes to better than $\pm 5^\circ$ azimuth at slant ranges in excess of 1500 m. The system consumes 1.1 W when active and is capable of entering a low-power 10 mW sleep mode sufficient to maintain its time base.

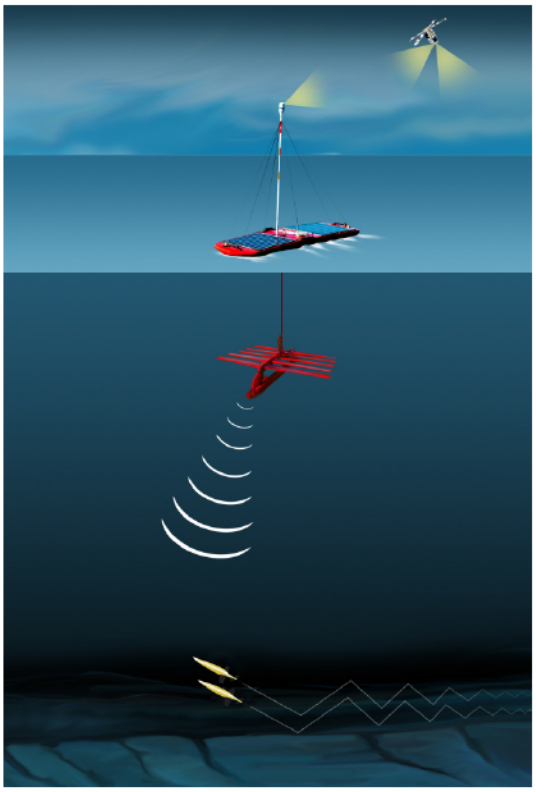

Fig. 1. Conceptual image of a OWTTIUSBL-based system showing a ASV providing acoustic range and position information to a fleet of gliders.

Figure 1 illustrates how OWTTIUSBL could support multi-glider operations. A fleet of gliders operates at depth while an ASV is on the sea surface. All of the subsea vehicles are equipped with a precision clock that provides a common low-drift time base synchronized to GPS time. At predefined intervals, the ASV transmits an acoustic data packet containing its GPS position along with the time the data packet was transmitted. Each glider is equipped with an acoustic array that measures the azimuth and elevation angles of the arriving packet relative to the array. The accurate time base afforded by precision clocks enables each glider to compare the time it received the data packet with the time it was sent and use this to compute a range. This measurement (effectively, the position of the ASV relative to the glider in spherical coordinates) can be transformed to Cartesian coordinates, rotated into the local-level frame using the submerged vehicle's attitude sensor,

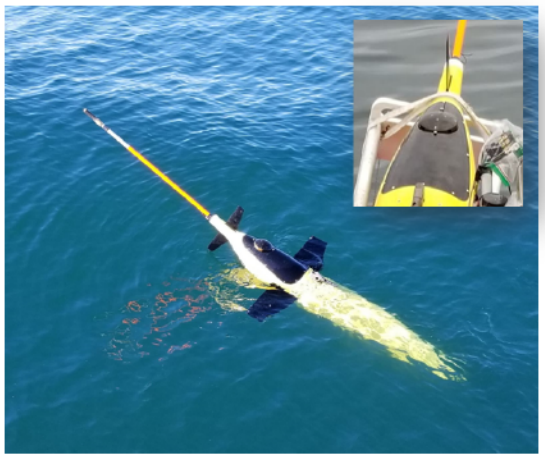

Fig. 2. A Seaglider with the OWTTIUSBL system installed during trials in November 2020. The inset shows the array. All four elements are visible.

and finally combined with the transmitted GPS position of the ASV to yield the geo-referenced position of the subsea vehicle with a single acoustic transmission.

We originally presented our concept at this conference in 2015 [1], along with predictions for achievable accuracy and the impact of the system on glider endurance. In this update we describe the realized system and report its performance as observed during field trials in November of 2020. Field trials consisted of deployments with the OWTTIUSBL integrated onto a Seaglider (Fig. 2) and mounted on the ship's CTD rosette cage. Long-baseline (LBL) acoustic transponders provided ground truth for comparison with the OWTTIUSBL.

II. Background

Disparities in size, available energy, cost, and operating domains result in navigation solutions employed by underwater robots that vary enormously. High-power propeller-driven survey AUVs typically use Doppler velocity logs (DVLs) and inertial navigation systems (INSs) combined with external position measurements, e.g., ultra-short-baseline (USBL) or LBL, while gliders, which must use low-power sensors, typically depend on surface GPS measurements and suffer more rapidly degraded navigational accuracy while submerged. In a few cases, gliders have been aided by acoustic means, when overlying ice and/or sustained monitoring activity justified the logistical overhead of permanent mooring-based [2] or semi-permanent ice-tethered [3] acoustic navigation infrastructure.

Conventional range measurements are based on the two-way acoustic travel time between the vehicle and sources. The use of one-way travel time (OWTT) methods eliminates the need for the receiver to transmit, instead enabling the receiver (e.g., the vehicle) to estimate ranges based on the one-way travel time of acoustic modem data packets that contain the time of origin as well as the position of the transmitting source [4].

A further reduction in the overhead of range-aided navigation is attained by relying on only a single acoustic source. Previous work by the authors [5], [6] and others, e.g., [7], [8], has demonstrated the feasibility single-source range-aided navigation. Single-source methods suffer from two principal deficiencies: (1) acoustic data must be accrued over time and fused with dead-reckoned odometry (e.g., DVL/INS) and (2) range estimates from a variety of relative bearings between the source and the receiver must be attained to provide a suitable navigation fix [9], [10], [11], [12]. This is a challenge in deep water because large distances must be traversed to create significant changes in relative bearing.

In contrast, a conventional USBL system requires bi-directional ranging but provides a full navigation fix from a single source with every ping. A receiver array resides on a surface vessel so that the range and relative azimuth and elevation can be fused with the location of the ship (i.e. GPS). The underwater vehicle must expend energy to reply to each interrogation from the surface, and coded messages or other means of sharing the acoustic channel must be used to differentiate interrogations and replies from multiple vehicles, which limits scalability.

Similar in concept to conventional USBL systems, an inverted USBL (IUSBL) system architecture inverts the role of the surface vessel and underwater vehicle such that the acoustic cycle originates subsea rather than on the surface vessel. The surface vessel replies to each interrogation with a message that includes its position. The underwater vehicle computes the range, azimuth and elevation to the surface vessel upon receipt. Previous work includes efforts to develop and field IUSBL systems [13], [14] and research in developing algorithms for fusing IUSBL measurements with strapdown navigation sensors (e.g., [15], [16]). As with range-only OWTT navigation, the addition of precision timing, i.e. OWTTIUSBL, eliminates the need for the underwater vehicle to transmit. This eliminates the power consumption associated with acoustic transmission and scales well to multiple underwater assets because the channel is effectively shared by all assets simultaneously.

The advantages of OWTTIUSBL navigation in the specific contexts of low cost and multi-vehicle operations have been recognised by others. Rypkema et al. [17] describe the first OWTTIUSBL system successfully implemented on a low cost AUV. In [18] they demonstrate the value of the system in a multi-AUV context where the OWTTIUSBL-equipped vehicles follow trajectories relative to a mobile source. The technique avoids the need to transmit the absolute position of the source and therefore avoids the need for an acoustic modem, making it especially well-suited to low-cost platforms.

The device described here could operate in the same way, but includes a modem which ostensibly will allow OWTTIUSBL-equipped vehicles to navigate in a geodetic coordinate frame. In a minimal OWTTIUSBL implementation the source cannot know the position of any subsea vehicles. Subsea navigation in a geodetic coordinate frame becomes valuable if the source's motion is constrained or to coordinate motion using knowledge of the source's mission plan.

Fig. 3. The OWTTIUSBL head consists of the array with integral preamplifier with a small housing containing a MEMS AHRS rigidly bolted to its underside. The acoustic processing electronics were located inside the Seaglider's main pressure housing.

III. OWTTIUSBL System Design

The OWTTIUSBL system consists of a topside transmitter and a subsea receiver (Fig. 3). The acoustic processing for both the topside system as well as the subsea system is performed by an underwater acoustic modem (the WHOI Micromodem-2 [19]) operating as a general-purpose acoustic processor.

A. Topside Transmitter

The acoustic navigation signals were transmitted from a WHOI Micromodem deckbox connected to a transducer towfish on a 50-foot cable, deployed over the side of the ship, or over the side of the small boat, depending upon the experimental trial. In future work, the transmitter will be a WHOI Micromodem-2 that has previously been integrated into a Liquid Robotics SV3 Wave Glider ASV.

The navigation signals were linear frequency-modulated sweeps, centered at 25 kHz with 5 kHz of bandwidth (i.e. a frequency range from 22.5 kHz to 27.5 kHz). The sweep duration was 40ms, giving a time-bandwidth product of 200 and potential matched-filter processing gain of up to 23 dB. The sweeps were aligned with a GPS-synchronized pulse-per-second to allow one-way travel time (OWTT) ranging, and we used a sweep repetition rate of 4 Hz. The transmit source level was approximately 185dB re:1μPa, although for the closest ranges we did reduce the transmit level to prevent analog saturation on the receiver, which would have distorted the USBL phase estimates.

For these experimental trials, the navigation signals were transmitted simply in a long train of sweeps at a 4 Hz repetition rate, giving a OWTT with a range ambiguity of approximately 375 m. The range ambiguity was resolved in post-processing by tracking ranges and determining consistent range estimates. In a fully autonomous deployment, the ASV-based transmitter would precede the train of navigational sweep signals with an acoustic packet containing the ASV GPS position and transmit time, to allow the glider to resolve potential OWTT range ambiguities autonomously in real time.

B. Subsea Receiver

The subsea receiver is designed to be modular, low-power, and easily integrated with various types of autonomous vehicles. It consists of a receive array rigidly mated to an AHRS inside a small pressure housing, cabled to a processor unit with a stable clock that are inside the vehicle pressure housing.

The array is an upward-looking four-element broadband ceramic hydrophone array with integrated preamplifiers, all potted in a urethane disc [20], with a syntactic foam backing upgraded to a 6000 m depth rating for this application. The hydrophones are arranged in a square with a 38 mm diagonal axis. The axes of the hydrophone array are oriented along-axis of the Seaglider and across-axis of the Seaglider. The array was pitched with respect to the glider by 16° so that the array is approximately level when the glider is diving.

A small pressure housing is rigidly bolted to the array's backing plate and contains a Sparton M2 MEMS AHRS. The AHRS axes are aligned with the hydrophone array axes. Tight mechanical integration of the AHRS with the array avoids the need for vehicle-specific calibration of offsets (a magnetic calibration is still required but requires no external reference).

To enable one-way travel-time measurement, the subsea system uses a Seascan temperature-compensated clock connected to the acoustic processor.

The acoustic receiver processor is again a WHOI Micromodem-2, with a four-channel analog signal conditioning and analog-to-digital sampling board.

The hydrophone signals were sampled simultaneously at 80 kSamples/sec, then digitally demodulated and basebanded to 10 kSamples/second/channel complex data stream. The data stream is then matched-filtered with a filter replica set to be the transmitted linear frequency-modulated sweep ("LFM") waveform. On the first of the four array channels, a peak detector with a threshold test is run on the output of the matched filter. When a detection peak occurs, the outputs of all four channels of complex matched filters is saved at the same baseband sample where the detected peak occurred. The complex phases are then used in a two-dimension search over angles of arrival to provide the angle of arrival estimates in the array frame.

C. Subsea Power

A primary goal of the OWTTIUSBL system design was to produce a low-power subsea unit for integration onto power-constrained platforms such as gliders. All of the acoustic transmissions occur on the surface vehicle, where power is relatively unconstrained, for example using solar power on Wave Gliders or generators on ships. The measured power of the subsea receiver system is just under 1.1 W (see Table I).

To maintain a synchronized clock for one-way travel time measurements, the Seascan clock must be powered continuously. The Seascan clock itself consumes about 3 mW,

Component	Power	Can Power Off?
Micromodem-2	465 mW	Yes
Multichannel Analog	385 mW	Yes
AHRS w/interface board	165 mW	Yes
Hydrophone Array	66 mW	Yes
Seascan w/interface board	7.5 mW	No
Total	**1088 mW**	**8 mW**

TABLE I
POWER CONSUMPTION OF SUBSEA OWTTIUSBL SYSTEM.

with an additional 4.5 mW for an interface board (WHOI-205122) that eases vehicle integration by allowing a wide input voltage range (up to 34V) and also converts from a single-wire open-drain "SAIL" serial bus to a more standard logic-level UART serial port, with Seascan serial control and parsing implemented on the Micromodem.

The remaining 1.08 W is for the iUSBL acoustic angle estimation, and can be powered off when not in active use. The Sparton M2 AHRS datasheet specifies its power consumption as 60mW. We added an interface board (WHOI-205137), again to ease vehicle integration by increasing the input voltage range, converting to RS232 UART serial port levels, and supplying the AHRS reflashing pins to the pressure housing's underwater bulkhead connector.

In previous deployments, we used a Microsemi Chip-Scale Atomic Clock (CSAC) as the subsea stable timebase, with a drift rate of approximately 1 ppb, compared with approximately 20 ppb for a Seascan. The power consumption of a CSAC is 120 mW for the clock alone, compared with 3 mW for the Seascan clock (and 7.5 mW for the Seascan clock with the WHOI-205122 interface board). Underwater gliders typically have relatively short dives (of order several hours), and very constrained energy budgets. Since the subsea clock can be re-synchronized with GPS at each surfacing, but cannot be power-cycled during dives, we selected the Seascan clock for Seaglider integration, with its higher drift rate but significantly lower power relative to the CSAC.

IV. FIELD TRIALS

We conducted two rounds of field trials with the OWTTIUSBL device integrated into a test article (Fig. 4) prior to a final field trial with the device integrated into a Seaglider. The overall objectives of the first two trials were to independently characterize the performance of the array itself and several candidate micro-electrical-mechanical systems (MEMS) AHRSs. These early trials established that the error budget was dominated by angle estimates the array, after magnetic calibration of the AHRSs. The trials described below were the first for which the selected AHRS and array were fully integrated into a target platform. To assess the performance of the integrated system we compared position fixes from the OWTTIUSBL to ground truth navigation provided by LBL transponders. The subsequent sections provide additional detail on the Seaglider trials and results.

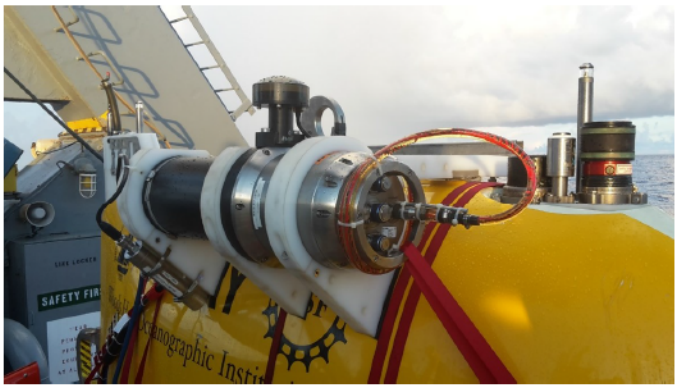

Fig. 4. The OWTTIUSBL test article mounted on the NDSF AUV *Sentry* for field trials in 2018. An iXBlue Phins fiber-optic north-seeking gyrocompass is rigidly mounted to one endcap of the housing. Several candidate AHRSs and the array were mounted to the same endcap to enable precise comparison of the AHRS data to ground truth provided by the Phins and to transform array angles into local-level coordinates.

A. Santa Monica Basin Cruise Plan

Field trials were conducted 15-19 Nov. 2020 from the *R/V Oceanus*, in the Santa Monica Basin, off the coast of southern California. This location was chosen for its deep water (900 m) and relatively protected operating area, where we were most likely to be able to carry out small boat operations in November. Our primary operating plan was to deploy the glider and use an over-the-side transducer to broadcast message for the iUSBL from a ship-based WHOI Micromodem deckbox. Due to a failing glider pump, we also performed what we refer to here as *lowerings*, where the glider hull and iUSBL array were attached to the CTD rosette, as shown in Figure 5. This enabled us to lower the instrument and record data at full water depth. In this case, to achieve horizontal separation from the glider and the surface transducer, we used a small boat to host the WHOI Micromodem and over-the-side transducer, with a co-located GPS. Two LBL transponders were deployed and used to provide ground truth of the glider position.

Table II shows a summary of the glider deployments and dives; Table III shows a summary of the missions where the glider hull and iUSBL array were strapped to the CTD frame and lowered into the water column.

B. LBL Transponders

To provide navigation against which to compare the OWTTIUSBL results, we deployed two 10 kHz LBL transponders on a baseline offset by about 1 km from the intended dive locations. Transponder surveys yielded sub-meter residuals in surveyed location. Limitations with respect to available transmit and receive frequencies on the glider forced the use of relay paths rather than conventional direct ranging. Acoustic travel times corresponded to the direct range between the ship and the glider, and relay paths from ship to transponder to glider and back to ship. Subsequent processing for ground truth navigation included sound speed profile correction from a conductivity-temperature-depth (CTD) cast conducted on site.

Start Date	Mission	Dive ID	Duration (min)	Depth (m)
15 Nov 2020	01	001	23	72
		002	32	110
		003	47	170
		004	114	384
		005	117	380
		006	286	895
		007	316	894
		008	42	116
16 Nov 2020	02	001	43	78
		002	45	98
19 Nov 2020	03	001	23	68
		002	33	108
		003	41	138
19 Nov 2020	04	001	33	105
		002	112	429

TABLE II
SEAGLIDER DEPLOYMENTS.

Date	Lowering	Duration (min)	Depth (m)
17 Nov 2020	01	19	188
17 Nov 2020	02	*faulty data collection*	
18 Nov 2020	03	64	400
18 Nov 2020	04	72	885
18 Nov 2020	05	153	885

TABLE III
SEAGLIDER LOWERINGS (GLIDER BODY STRAPPED TO CTD CAROUSEL).

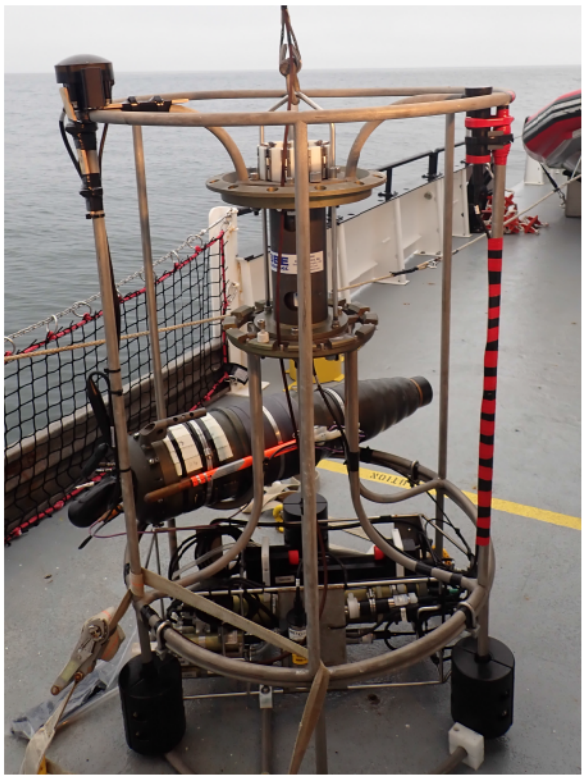

Fig. 5. Data from glider "lowerings" were collected with the Seaglider hull strapped to the inside of the CTD rosette frame, seen here on the far side of the rosette frame, with the iUSBL mounted on the top rail (upper left).

Fig. 6. Photo of dock test angle calibration rig, with iUSBL receiver on left, reference transducer on right, with both azimuth and elevation angle adjustment jigs. The device will be motorized to permit in situ scanning across azimuth and elevation.

C. Glider "Lowerings"

While not in the original cruise plan, having the glider hull and array attached to the CTD rosette (see Fig. 5) provided the opportunity to capture valuable calibration data. The CTD depths and small boat locations were carefully selected to collect datasets where, for example, we independently varied the horizontal and vertical distance between the glider and the surface transducer; tested the maximum range or maximum slant angle; and collected data in a full circle around the array. We culminated with an attempt to trace out the letters "OWTT" with towfish transmitter deployed from the small boat to see how well the iUSBL could recreate the position of the small boat during the maneuvers (while also testing the small boat skills of the R/V Oceanus crew).

V. DEVICE PERFORMANCE

This section presents an overview of downstream processing applied to travel time and arrival angle data to arrive at a position fix, followed by an analysis of single-fix standalone navigation performance, primarily as a function of the position and orientation of the array relative to the source. Quantitative results are presented from the CTD cage "lowerings" described above. We conclude with preliminary results from a Seaglider dive.

A. OWTTIUSBL Navigation

The OWTTIUSBL device is intended to provide nearly stand-alone position fixes to host platforms. This approach trades the potential accuracy gains of tightly-coupled approaches [16], [17] informed by vehicle motion in favor of streamlined integration. The detection and beamforming process described in Sec. III yields a travel-time and a unit vector encoding the arrival direction. The unit vector can alternatively be expressed as an array-frame azimuth and elevation. For a level array oriented about the vertical such that its primary horizontal axis points north, the array-frame

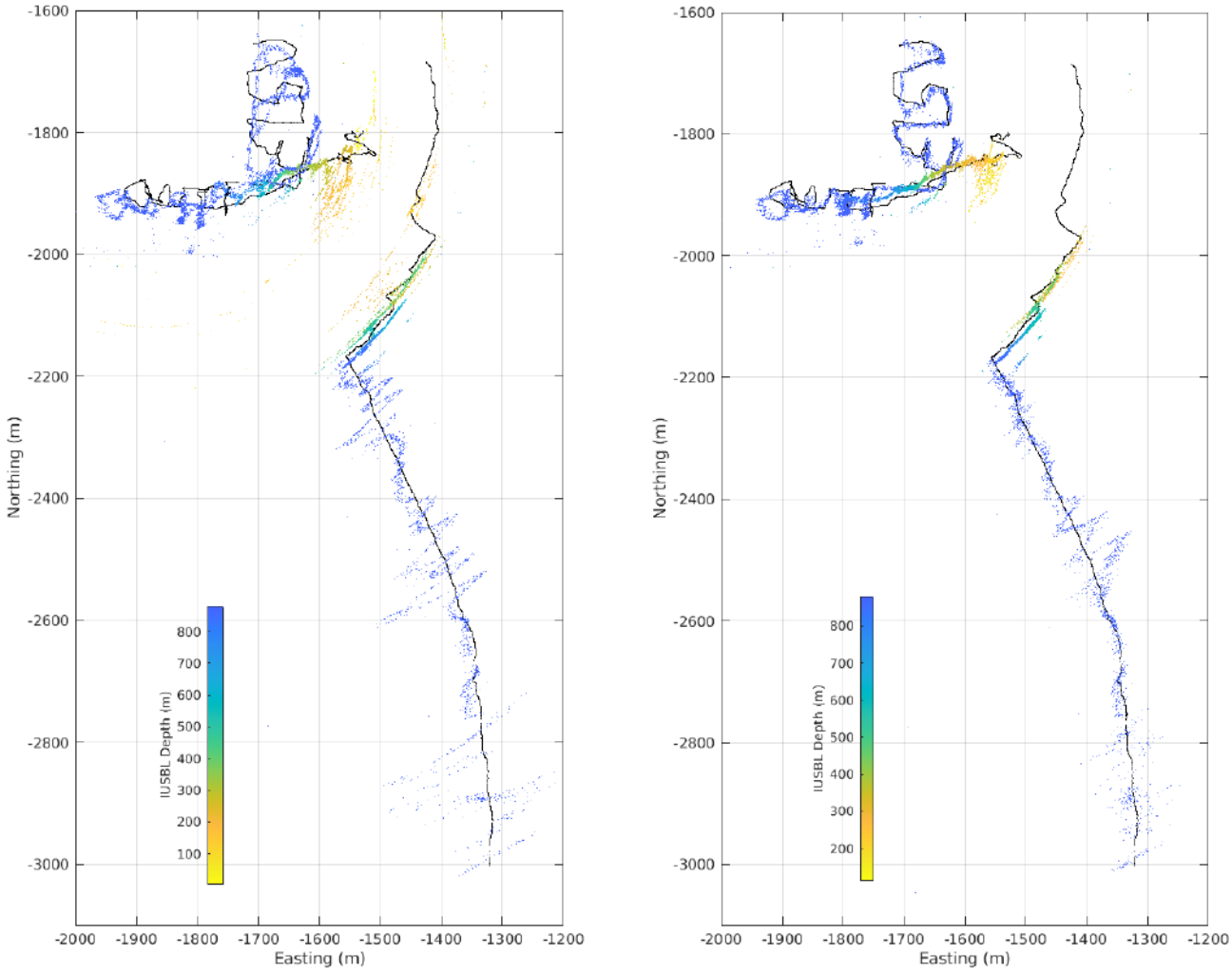

Fig. 7. Transmitter position as computed from uncompensated (left) and compensated (right) OWTTIUSBL data with the device mounted on the ship's CTD cage. Fix color indicates depth of the cage. LBL positioning provided ground truth for the location of the cage, which wandered a few 10s of m about approximately $(-1900, -1700)$. The ground truth position of the transmitter, carried aboard the ship's small boat during the test, was determined using GPS positioning and is rendered in black. The letters "OWTTIUSBL" appear in upper left, as executed by the small boat. The letters are significantly more distinct in the compensated results.

angles equal the celestial azimuth and elevation. These data, along with an estimate of sound speed profile, are sufficient to compute a stand-alone fix; however, the beampattern of the array yields relatively noisy estimates of array-frame elevation, except at angles approaching 90° (straight out from the face of the array).

For array attitudes near level, a superior position estimate is attained by combining array-frame azimuth with celestial elevation derived from acoustic range and vehicle depth. This approach discards the information in the component of the unit vector facing out of the array. The solution is not strictly standalone since it relies on an external depth measurement, but high accuracy depth measurements are ubiquitous on underwater robots.

The azimuth-only solution works well for limited tilt. We chose to prioritize positioning performance during descents and installed the array on the Seaglider such that its orientation is near-level as the glider descends. During ascents, the tilt is potentially large; we observed upwards of 40° during field trials. At large tilts, and depending on the relative positions of the surface source and glider, certain orientations of the glider can prevent detection altogether or yield poor angle estimates. The CTD cage data is ostensibly representative of positioning performance during descents. Circumstances conspired to limit the OWTTIUSBL data collected on the Seaglider to primarily a single ascent from 400 m.

The OWTTIUSBL can provide position fixes even at high tilt, but to do so requires additional processing. At high tilt the azimuth-only equations admit two solutions, both of which are geometrically admissible. At relatively large hori-

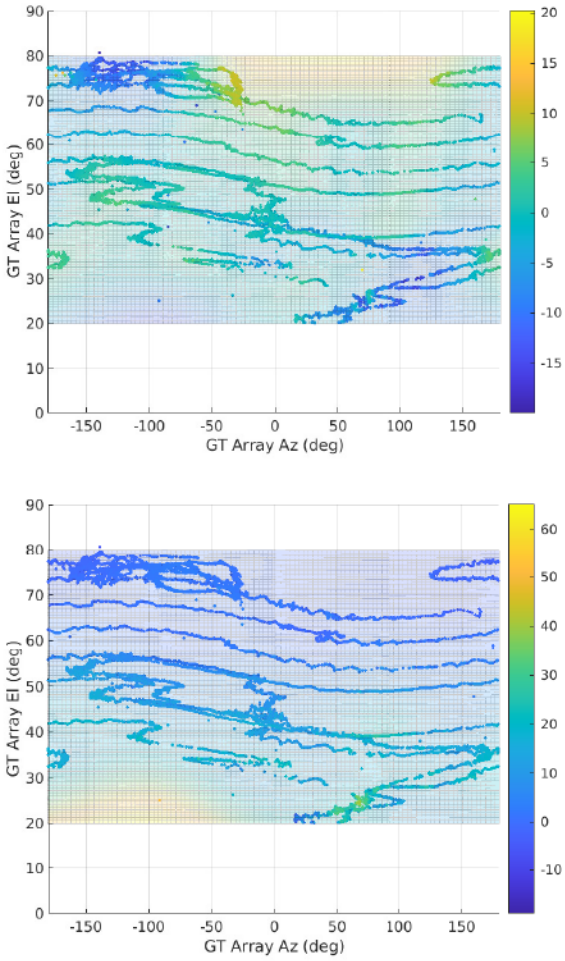

Fig. 8. Array calibration results from CTD cage lowering 05 (top: azimuth error; bottom: elevation error). All data are transformed into the array-frame. The meshes depict error surfaces fit to the data and used subsequently to compensate measured arrival angle. Colors depict error in degrees. Data outside the interval $[20°, 80°]$ was sparse and inconsistent. Regions in the interval but with sparse data tend to result in large and unrealistic excursions in the fitted error surface.

zontal displacements between source and receiver, one solution corresponds to a arrival direction vector with a component pointing out of the back of the array and can be discarded. At relatively small horizontal displacements, additional data are needed to select between solutions, for example, the measured array-frame elevation, or output from an estimation filter. At high tilts the azimuth-only solution is sensitive to the relative position and orientation of the array to the source. We found it effective to compute the partial derivative of the computed celestial azimuth with respect to the array-frame azimuth and then discard data exceeding a threshold. This discards solutions with high sensitivity to noise or bias in measured array-frame azimuth.

B. Cabled Results

Installing the glider on the CTD cage allowed us to excite the OWTTIUSBL array over a large range of array-frame azimuth and elevation and assess performance as a function of both. This was achieved by lowering the CTD cage to depth and then driving the ship's small boat on a radial trajectory with the acoustic source towed slowly behind, out to a distance of about 1500 m from the ship (Fig. 7). The CTD cage spun slowly throughout the experiment, which served to vary array-frame azimuth of the source.

The left panel of Fig. 7 shows raw OWTTIUSBL fixes and captures artifacts that we believe are systematic biases introduced by the construction of the array. These appear to dominate the random noise. As such it should be possible to apply an array calibration to compensate. An independent calibration awaits completion of an active rig (Fig. 6). Here we present preliminary results using the CTD cage data itself to determine a calibration. This approach is clearly prone to overfitting, and therefore potentially optimistic; however, there are good reasons to believe the calibration does capture distortions introduced by the array.

Fig. 8 shows the error in measured array-frame azimuth and elevation with ground truth derived from LBL positioning of the CTD cage, and GPS positioning of the source. A compensation is computed by fitting a surface to these points while imposing a smoothness criterion.[1] For the interval of ground truth array-frame elevations depicted in the figure, there is obvious correlation in the errors between nearby samples, including on multiple nearby "passes" resulting from rotation of the CTD cage—these show up on the plots as small-amplitude undulations in elevation versus azimuth. This suggests the errors observed are not strongly time-dependent, but rather functions of true array-frame arrival direction.

The array-frame azimuth error surface depicted in the upper panel of Fig. 8 was subtracted from the measured array-frame azimuth to produce the compensated result in the right panel of Fig. 7. To do so directly would require knowledge of the true array-frame azimuth and elevation, neither of which are known without an independent source of navigation. Instead we used the measured array-frame azimuth, and the derived array-frame elevation computed from array-frame azimuth, depth, and range, in place of ground truth versions of the same. This works best for small tilts and assumes the distortions in array-frame azimuth vary slowly as a function of true array-frame azimuth.

There are distinct differences between the raw and compensated results in the panels Fig. 7. Both results show broad agreement with ground truth. The compensated results better resolve the small scale features (letters) in the upper left of the plot, evidence fewer across-track oscillations on the southeast radial leg, and smaller deviations in the circumferential direction, particularly for the shallow data. These may all be explained by array-induced distortions periodic in true azimuth and manifested through slow rotation of the CTD cage. Biases occur primarily in the circumferential direction because celestial elevation is well-constrained by depth and

[1]https://www.mathworks.com/matlabcentral/fileexchange/8998-surface-fitting-using-gridfit

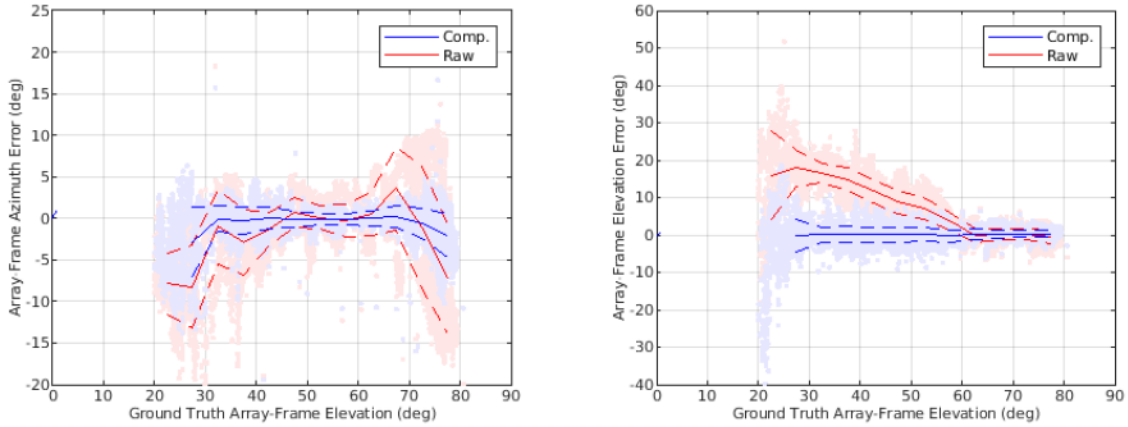

Fig. 9. Measured array-frame azimuth and elevation error as a function of ground truth versions of the same for both raw and compensated data. Solid and dashed lines depict the mean error and standard deviation thereof, binned in 5° increments. Note the scale is not the same between the panels—elevation is generally noisier.

range.

For lack of an independent calibration our results must be considered preliminary. For this reason, we present in Fig. 9 summary performance for both uncompensated and compensated data, and contend the former represents a worst case. Both array-frame azimuth and elevation become dramatically noisier at true array-frame elevations below about 30°. The array design, particularly the syntactic foam backing likely distorts incoming sound for these low elevations. This was expected. In light of the target deep water navigation application we traded better high-elevation performance at the expense of degraded low-elevation performance. At high array-frame elevations the array-frame azimuth estimate degrades, a function of both trigonometry and the array's beam pattern, whereas the array-frame elevation estimate improves. The impact of degraded azimuth estimation on navigation performance is limited at high angles where depth and range provide a powerful constraint, nevertheless, the array clear performs best at intermediate angles We do not as yet have an explanation for the large systematic bias in array-frame elevation visible for elevations below 60°, however, the measured array-frame elevation is presently discarded when computing fixes (Sec. V-A).

Based on Fig. 9, the system is capable of providing standalone fixes to better than ±5° in azimuth at low tilts and for elevations between about 30° to 70°, without compensating for array-induced distortions. This corresponds to a horizontal position uncertainty, primarily in the circumferential direction, of, e.g., ±100 m at 1000 m depth and 1000 m horizontal displacement. Error is dominated by bias in arrival angle estimation. Our previous analyses [1] predicted attitude error would dominate the error budget; that analysis proved optimistic with respect to array performance. The ultimate performance of the system may be substantially better than that achieved so far. Random noise in the arrival angle estimate is readily diminished by averaging, and for slow platforms short bursts at high rate would not require knowledge of platform motion. Bias cannot be attenuated by averaging, but a planned high-resolution array calibration (Fig. 6) may shed more light on the sources of bias and yield an improved compensation.

C. Seaglider Results

For the Seaglider results, we present an analysis from Dive 002 of Mission 04. During this dive, which lasted 112 minutes, the glider performed a spiral descent and ascent, and reached a maximum depth of 429 meters. The spiral, while not a typical dive path, was chosen to keep the glider within the limited range of the LBL beacons. The surface transducer was lowered over the side of the ship.

a) Ground Truth Navigation: We calculated the ground truth Seaglider trajectory using an extended Kalman filter with a constant velocity process model [3], ingesting both direct range measurements from the ship to the glider, and relayed range measurements as described in IV-B. Returns from transponder 1 were unreliable and inconsistent, and thus were omitted. The range measurements are based on the round trip time-of-flight along the given path, corrected for the depth varying sound speed along that path. In addition, current data from the OS75 ADCP onboard the R/V Oceanus was incorporated into the solution to correct for advection of the glider during its dive.

The constant velocity process model employed to calculate the ground truth is better suited to long straight trajectories, as opposed to the spiral dive employed here. As a result the ground truth trajectory appears less smooth than expected. This is exacerbated during the periods of the dive when the sampling period increases from 5 or 10 seconds to 30 seconds. In future work, the ground truth trajectory will also be smoothed.

b) OWTTIUSBL: Fig. 10 shows the best-estimate ground truth navigation described previously along with independent position fixes from the OWTTIUSBL device. The data shown corresponds to an ascent from approximately 450 m. During

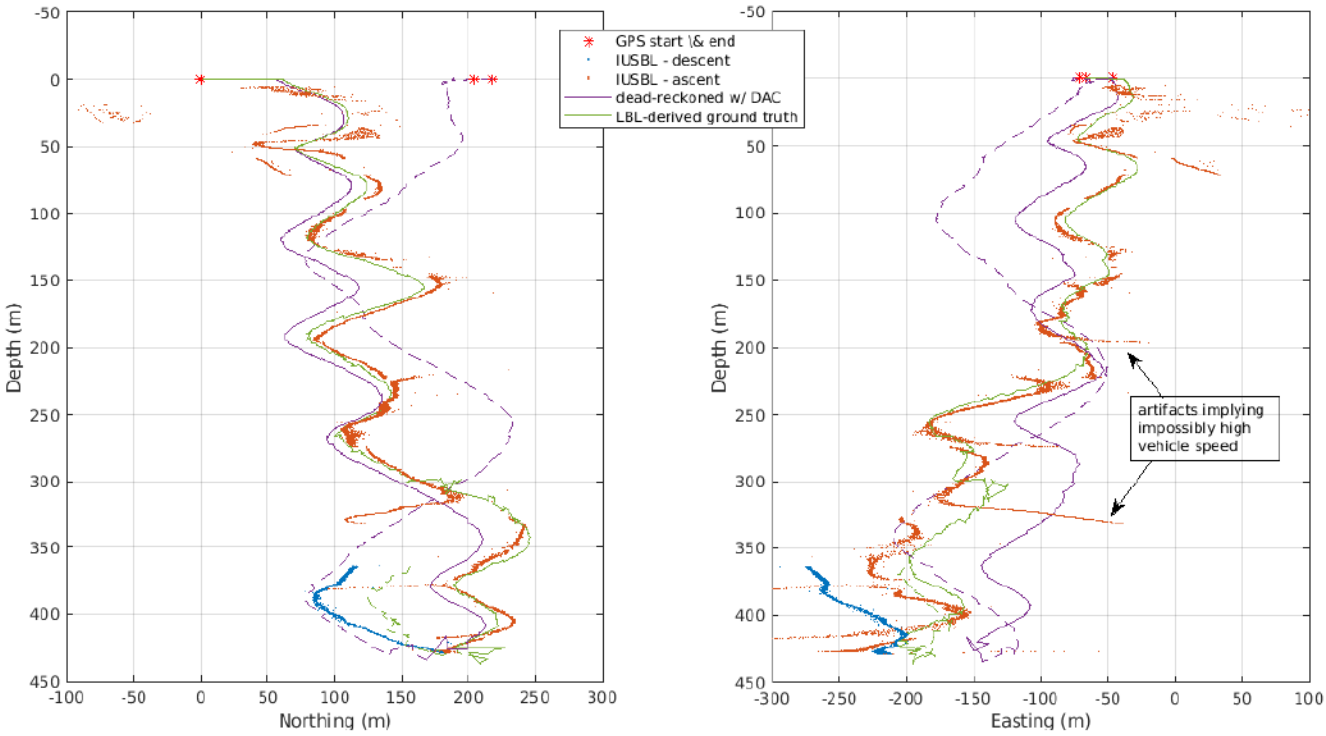

Fig. 10. Two views of Seaglider dive 002 from mission 04 comparing OWTTIUSBL position fixes against LBL-derived ground truth and conventional (post-dive) depth-averaged current glider navigation. The source was at the surface and holding station (live boating) at a position roughly centered on the glider trajectory. Labeled features are discussed in the text.

ascents the OWTTIUSBL device is pitched at about 40° and therefore typically produces lower quality fixes relative to performance at low tilts. For this dive the geometry was such that the array-frame azimuth-only solution also often returned dual feasible solutions. Despite these factors, the OWTTIUSBL position fixes align reasonably well with ground truth at times, especially at intermediate depths between 50 m and 300 m. This result relies on the application of self-contained single-fix metrics for fix rejection and selection between possible solutions as described in Sec. V-A. Fixes for which the sensitivity of the computed celestial azimuth to measured array-frame azimuth exceeded a factor of two were discarded. Dual solutions were disambiguated by selecting the solution whose derived array-frame elevation more closely matched the measured array-frame elevation. Some obvious artifacts remain, particularly strings of fixes lying on near-constant depth arcs that imply a velocity far in excess of that achievable by a Seaglider. More sophisticated metrics for fix rejection could therefore be employed, but the result shown here is self-contained and agnostic to host platform.

The figure also contains a short portion of the glider's descent near apogee. During this portion of the dive the array is near level and the geometry ideal. The fixes are spatially concentrated and markedly free of artifacts in contrast to the ascent. The shape of the trajectory is locally very similar to the dead-reckoned trajectory compensated for depth-averaged current (DAC). This suggests good OWTTIUSBL fixes—dead reckoning is accurate over short intervals. However, the match to LBL-derived ground truth is poor. The reason for this discrepancy remains unclear but it may be that the LBL ranges temporarily corresponded to a bounce path or suffered some other distortion.

The OWTTIUSBL fixes from the ascent are noisy and not well-suited to autonomous navigation; however, their value is significant when compared to conventional glider navigation, which cannot account for the water current profile in real time. Differencing the GPS position upon surfacing from that predicted by dead-reckoning yields a correction in post-processing, and is equivalent to assuming a constant, uniform water current profile with a magnitude and direction known as the depth-averaged current [21]. This approach cannot account for temporal or depth variability in the current profile. Fig. 10 shows a DAC-compensated trajectory estimate that compares reasonably well with the ground truth and OWTTIUSBL results when looking east (left panel). All solutions indicate a southward drift confirmed by surface GPS fixes. Viewed looking north (right panel), the DAC-compensated trajectory fails to capture a slight eastward drift in the upper water colum above 200 m and a more significant westward drift below 200 m. In principle, the current profile could be resolved

as the disparity between dead-reckoned OWTTIUSBL-derived trajectory estimates. For applications requiring real-time subsea navigation the DAC-compensated solution is not available and the value of external aiding increases.

VI. Implications and Plans

Development of the OWTTIUSBL system continues. Results to date are sufficient to compute position fixes in post-processing but not in real time. To do so will require interlacing messages containing ephemeris and timing data with the USBL signal, as well as subsea processing to fuse acoustic and attitude data, and algorithm development to robustly reject outliers. Integration of the OWTTIUSBL into another Seaglider is underway in preparation for a multi-vehicle demonstration in early 2022. The system is also being integrated into a REMUS 600 AUV and a modified hybrid Slocum glider. The system can and has been configured to receive at 10 kHz instead of 25 kHz in anticipation of deployments on deeper-diving vehicles. While this improves range, it also reduces the accuracy of the angle estimates.

OWTTIUSBL could have a profound impact on deep-diving gliders, long-range AUVs (LRAUVs), as well as enabling new operational paradigms for conventional deep-diving AUVs. It could enable deep-diving gliders to perform new missions such as extended hydrothermal vent surveys along mid-ocean ridges, and multi-day (or longer) deep-water physical oceanographic profiling missions; as well as provide a foundation for teams of LRAUVs and an attending ASV to undertake basin-scale surveys of the seafloor with improved navigation and a vastly reduced need to surface.

Acknowledgements

This research was supported by NSF awards OCE-1634298 (WHOI) and OCE-1634286 (APL-UW); and the NOAA Office of Exploration and Research award NA18OAR0110356.

The authors would like to thank the captain and crew of the R/V Oceanus, as well as the OSU Marine Operations team for their extensive support with cruise scheduling and logistics during the pandemic. The authors would also like to thank the captains and crews of the R/V Atlantic Explorer and R/V Okeanos Explorer, as well as the Deep Discoverer ROV team for their support on previous cruises during the development of the array.

The authors gratefully acknowledge Geoff Shilling for assistance with glider piloting, Jason Gobat for assistance with Seaglider integration, and Nick Rypkema for providing insights into array performance and beam pattern.

References

[1] M. V. Jakuba, J. C. Kinsey, J. W. Partan, and S. E. Webster, "Feasibility of low-power one-way travel-time inverted ultra-short baseline navigation," in *OCEANS 2015-MTS/IEEE Washington*. IEEE, 2015, pp. 1–10.

[2] S. E. Webster, C. M. Lee, and J. I. Gobat, "Preliminary results in under-ice acoustic navigation for Seagliders in Davis Strait," in *Proc. IEEE/MTS OCEANS Conf. Exhib.*, St. John's, Sept 2014, pp. 1–5.

[3] S. E. Webster, L. E. Freitag, C. M. Lee, and J. I. Gobat, "Towards real-time under-ice acoustic navigation at mesoscale ranges," in *Proc. IEEE Intl. Conf. Robot. Auto.*, Seattle, WA, May 2015, pp. 1–8.

[4] R. M. Eustice, H. Singh, and L. L. Whitcomb, "Synchronous-clock, one-way-travel-time acoustic navigation for underwater vehicles," *Journal of Field Robotics*, vol. 28, no. 1, SI, pp. 121–136, Jan-Feb 2011.

[5] J. Kinsey, M. Jakuba, and C. German, "A long term vision for long-range ship-free deep ocean operations: persistent presence through coordination of autonomous surface vehicles and autonomous underwater vehicles," in *Workshop on Marine Robotics and Applications. Looking into the Crystal Ball: 20 years hence in Marine Robotics*, 2013.

[6] S. Webster, R. Eustice, H. Singh, and L. Whitcomb, "Advances in single-beacon one-way-travel-time acoustic navigation for underwater vehicles," *The International Journal of Robotics Research*, vol. 31, no. 8, pp. 935–950, 2012.

[7] M. F. Fallon, G. Papadopoulos, J. J. Leonard, and N. M. Patrikalakis, "Cooperative AUV navigation using a single maneuvering surface craft," *Intl. J. Robotics Research*, vol. 29, no. 12, pp. 1461–1474, Oct 2010.

[8] J. H. Kepper, B. C. Claus, and J. C. Kinsey, "A navigation solution using a MEMS IMU, model-based dead-reckoning, and one-way-travel-time acoustic range measurements for autonomous underwater vehicles," *IEEE Journal of Oceanic Engineering*, vol. 44, no. 3, pp. 664–682, 2018.

[9] A. Gadre and D. Stilwell, "A complete solution to underwater navigation in the presence of unknown currents based on range measurements from a single location," in *Proc. IEEE/RSJ Intl. Conf. Intell. Robots Systems*, 2005, pp. 1420–1425.

[10] P. Baccou and B. Jouvencel, "Simulation results, post-processing experimentations and comparisons results for navigation, homing and multiple vehicles operations with a new positioning method using on transponder," in *IEEE International Conference on Intelligent Robots and Systems*, vol. 1, Las Vegas, NV, United States, Oct. 2003, pp. 811–817.

[11] T. L. Song, "Observability of target tracking with range-only measurements," *Oceanic Engineering, IEEE Journal of*, vol. 24, no. 3, pp. 383–387, 1999.

[12] A. P. Scherbatyuk, "The AUV positioning using ranges from one transponder LBL," in *Proc. IEEE/MTS OCEANS Conf. Exhib.*, vol. 3, San Diego, CA, 1995, pp. 1620–1623.

[13] K. Vickery, "Acoustic positioning systems - new concepts: The future," in *Proceedings of the IEEE Symposium on Autonomous Underwater Vehicle Technology*, Cambridge, MA, USA, Aug. 1998, pp. 103–110.

[14] T. Hiller, A. Steingrimsson, and R. Melvin, "Expanding the small auv mission envelope; longer, deeper & more accurate," in *Autonomous Underwater Vehicles (AUV), 2012 IEEE/OES*. IEEE, 2012, pp. 1–4.

[15] P. Batista, C. Silvestre, and P. Oliveira, "GAS tightly coupled LBL/USBL position and velocity filter for underwater vehicles," in *Control Conference (ECC), 2013 European*. IEEE, 2013, pp. 2982–2987.

[16] M. Morgado, P. Oliveira, and C. Silvestre, "Tightly coupled ultrashort baseline and inertial navigation system for underwater vehicles: An experimental validation," *Journal of Field Robotics*, vol. 30, no. 1, pp. 142–170, 2013.

[17] N. R. Rypkema, E. M. Fischell, and H. Schmidt, "One-way travel-time inverted ultra-short baseline localization for low-cost autonomous underwater vehicles," in *2017 IEEE International Conference on Robotics and Automation (ICRA)*. IEEE, 2017, pp. 4920–4926.

[18] E. M. Fischell, N. R. Rypkema, and H. Schmidt, "Relative autonomy and navigation for command and control of low-cost autonomous underwater vehicles," *IEEE Robotics and Automation Letters*, vol. 4, no. 2, pp. 1800–1806, 2019.

[19] E. Gallimore, J. Partan, I. Vaughn, S. Singh, J. Shusta, and L. Freitag, "The whoi micromodem-2: A scalable system for acoustic communications and networking," in *Proc. IEEE/MTS OCEANS Conf. Exhib.*, Sept 2010, pp. 1–7.

[20] F. Jaffre, T. Austin, B. Allen, R. Stokey, and C. Von Alt, "Ultra short baseline acoustic receiver/processor," in *Proc. IEEE/MTS OCEANS Conf. Exhib.*, Brest, France, June 2005, pp. 1382–1385.

[21] D. Chang, F. Zhang, and C. Edwards, "Real-time guidance of underwater gliders assisted by predictive ocean models," *Journal of Atmospheric and Oceanic Technology*, vol. 32, pp. 562–578, 03 2015.